

University of Groningen

## Solubilities of sub- and supercritical carbon dioxide in polyester resins

Nalawade, SP; Picchioni, F; Janssen, LPBM; Patil, VE; Keurentjes, JTF; Staudt, R;  
Nalawade, Sameer P.; Patil, Vishal E.; Keurentjes, Jos T.F.

*Published in:*  
Polymer Engineering and Science

*DOI:*  
[10.1002/pen.20518](https://doi.org/10.1002/pen.20518)

**IMPORTANT NOTE:** You are advised to consult the publisher's version (publisher's PDF) if you wish to cite from it. Please check the document version below.

*Document Version*  
Publisher's PDF, also known as Version of record

*Publication date:*  
2006

[Link to publication in University of Groningen/UMCG research database](#)

### *Citation for published version (APA):*

Nalawade, SP., Picchioni, F., Janssen, LPBM., Patil, VE., Keurentjes, JTF., Staudt, R., Nalawade, S. P., Patil, V. E., & Keurentjes, J. T. F. (2006). Solubilities of sub- and supercritical carbon dioxide in polyester resins. *Polymer Engineering and Science*, 46(5), 643-649. <https://doi.org/10.1002/pen.20518>

### **Copyright**

Other than for strictly personal use, it is not permitted to download or to forward/distribute the text or part of it without the consent of the author(s) and/or copyright holder(s), unless the work is under an open content license (like Creative Commons).

The publication may also be distributed here under the terms of Article 25fa of the Dutch Copyright Act, indicated by the "Taverne" license. More information can be found on the University of Groningen website: <https://www.rug.nl/library/open-access/self-archiving-pure/taverne-amendment>.

### **Take-down policy**

If you believe that this document breaches copyright please contact us providing details, and we will remove access to the work immediately and investigate your claim.

*Downloaded from the University of Groningen/UMCG research database (Pure): <http://www.rug.nl/research/portal>. For technical reasons the number of authors shown on this cover page is limited to 10 maximum.*

# Solubilities of Sub- and Supercritical Carbon Dioxide in Polyester Resins

Sameer P. Nalawade, Francesco Picchioni, Leon P.B.M. Janssen

Department of Chemical Engineering, University of Groningen, 9747 AG Groningen, The Netherlands

Vishal E. Patil, Jos. T.F. Keurentjes

Process Development Group, Department of Chemical Engineering and Chemistry, Eindhoven University of Technology, 5600 MB Eindhoven, The Netherlands

Reiner Staudt

Institut für Nichtklassische Chemie, University of Leipzig, Permoserstrasse 15, 04318 Leipzig, Germany

In supercritical carbon dioxide (CO<sub>2</sub>) assisted polymer processes the solubility of CO<sub>2</sub> in a polymer plays a vital role. The higher the amount of CO<sub>2</sub> dissolved in a polymer the higher is the viscosity reduction of the polymer. Solubilities of CO<sub>2</sub> in polyester resins based on propoxylated bisphenol (PPB) and ethoxylated bisphenol (PEB) have been measured using a magnetic suspension balance at temperatures ranging from 333 to 420 K and pressures up to 30 MPa. An optical cell has been used to independently determine the swelling of the polymers, which has been incorporated in the buoyancy correction. In both polyester resins, the solubility of CO<sub>2</sub> increases with increasing pressure and decreasing temperature as a result of variations in CO<sub>2</sub> density. The experimental solubility has been correlated to the Sanchez-Lacombe equation of state. POLYM. ENG. SCI., 46:643–649, 2006. © 2006 Society of Plastics Engineers

## INTRODUCTION

Polyester resins in powder form are frequently used in paint and toner industry. Milling, grinding, and spray drying are the particle formation processes commonly used in the industry. Narrow particle size distribution, solvent recovery, and the prevention of volatile organic components (VOC) emission are the major challenges associated with these processes. Moreover, the classical processes have clear disadvantages in terms of energy requirement due to expensive cryogenic cooling, and problems with product quality due to heat dissipation during milling, which causes agglomeration by molten polymer particles. This has motivated chemical

engineers as well as chemists to adopt supercritical technologies in which the problems described above can be eliminated.

Unusual solvent properties above the critical point like gas-like diffusivities and liquid-like densities make supercritical technology attractive. Particles from gas saturated solution (PGSS) is one of the particle production methods using a supercritical fluid [1]. Supercritical carbon dioxide (CO<sub>2</sub>) has a high solubility in many polymers. In PGSS, the viscosity of the polymer, particle size, and morphology of the particles are mainly determined by the amount of CO<sub>2</sub> dissolved in the polymer. Therefore, it is important to determine the solubilities of CO<sub>2</sub> in a polymer at different conditions so as to define the processing window.

Various experimental methods exist to determine the solubility of CO<sub>2</sub> in solid and in molten polymers. Phase separation [2], volumetric [3], and gravimetric [4] methods are commonly used. In the first two methods, the amount of polymer required is large compared to gravimetric methods, and hence, the time required to reach equilibrium is substantially longer. Moreover, high accuracy in pressure sensors and volume measurements are required in the first two methods for solubility calculations. These disadvantages are overcome by a gravimetric method that uses a microbalance [4]. The principle behind the gravimetric method is the weight difference between a gas-free and a gas-sorbed polymer sample. With a microbalance of high accuracy, even a small change in the weight of the polymer sample due to dissolved gas can be measured. Recently, a magnetic suspension balance (MSB), developed by Kleinrahn and Wagner [5], has been used to measure the solubility of CO<sub>2</sub> in various polymers [6–8]. A major advantage of using the MSB is that measurements can be carried out at elevated

Correspondence to: L.P.B.M. Janssen; e-mail: L.P.B.M.Janssen@rug.nl  
DOI 10.1002/pen.20518  
Published online in Wiley InterScience (www.interscience.wiley.com).  
© 2006 Society of Plastics Engineers

TABLE 1. Physical properties of the polymers.

Polymers	$M_n$ (g/mol)	$M_w$ (g/mol)	$T_g$ (K)	$\eta_0$ at 363 K (Pa s)
PPB	2,700	7,000	325–329	2,965
PEB	8,500	20,000	328–332	47,540

temperatures and pressures without having direct contact between a sample and the balance.

The main objective of this work was to determine the solubilities of CO<sub>2</sub> in polyester resins using an MSB. An important parameter in such gravimetric measurements is the swelling of polymer due to dissolved CO<sub>2</sub>. A buoyancy correction due to swelling has to be taken into account while calculating the dissolved quantity of CO<sub>2</sub> in a polymer [6–8]. Therefore, an optical cell has been used in separate experiments to observe the swelling of polymers in the presence of CO<sub>2</sub> at similar conditions. The other objective of the study was to describe the solubility data using a thermodynamic model, the Sanchez–Lacombe equation of state (S-L EOS) [9, 10].

## EXPERIMENTAL PROCEDURES

### Materials

Polyester resins based on propoxylated bisphenol (PPB, CAS: 177834–94-5) and ethoxylated bisphenol (PEB, CAS: 170831–75-1) were obtained from Akzo Nobel, The Netherlands. The physical properties of the polymers are provided in Table 1. Both polymers are amorphous, which was confirmed by DSC measurements. The dry grade (> 99.5%) CO<sub>2</sub> was used for the measurements. All chemicals were used as-received without further purification.

### Apparatus and Method

**Magnetic Suspension Balance.** An MSB (Fig. 1) was used for measuring the solubility of CO<sub>2</sub> in both polymers. The MSB can be used at temperatures up to 473 K and pressures up to 50 MPa. A polymer sample was kept in a basket that was not directly connected to the weighing balance (microbalance), but was kept in place using a so-called suspension magnet. The suspension consists of a measuring load, a sensor core, and a permanent magnet. The measured weight of the basket containing the polymer was transmitted by a magnetic suspension coupling to an external microbalance, and thus, leak-proof measurements can be performed. In the MSB apparatus, the microbalance can be tare and calibrated during measurements. Using the MSB, the amount of CO<sub>2</sub> dissolved in a polymer was determined from the following relationship:

$$W_{\text{CO}_2} = \Delta W + \rho_{\text{CO}_2}(V_P(P, T, S) + V_B) \quad (1)$$

where  $\Delta W$  is the weight difference between a polymer sample in the absence of CO<sub>2</sub> at time  $t = 0$  and the same sample equilibrated with CO<sub>2</sub> at a desired temperature  $T$  and pressure  $P$  until a constant weight is obtained. The second term in Eq. 1 is a buoyancy correction term, which is required as polymers swell considerably in the presence of dissolved CO<sub>2</sub>.  $\rho_{\text{CO}_2}$ ,  $V_P(P, T, S)$ , and  $V_B$  are the density of CO<sub>2</sub>, the volume of the swollen polymer after contacting CO<sub>2</sub> with a solubility ( $S$ ), and the volume of the basket, respectively. As it was not possible to observe the polymer swelling simultaneously during the solubility measurements, an optical cell was used separately for the swelling measurements.

CO<sub>2</sub> solubility measurements were carried out above the glass-transition temperature ( $T_g$ ) of both polyesters. Temperature and pressure were varied from 333 to 420 K and 5–30 MPa, respectively. A polymer sample was first exposed to a vacuum for a few hours at the measurement temperature and an initial reading was recorded. This was followed by addition of CO<sub>2</sub> in the chamber until the desired pressure was attained. The sample was allowed to attain sorption equilibrium (in terms of the weight differ-

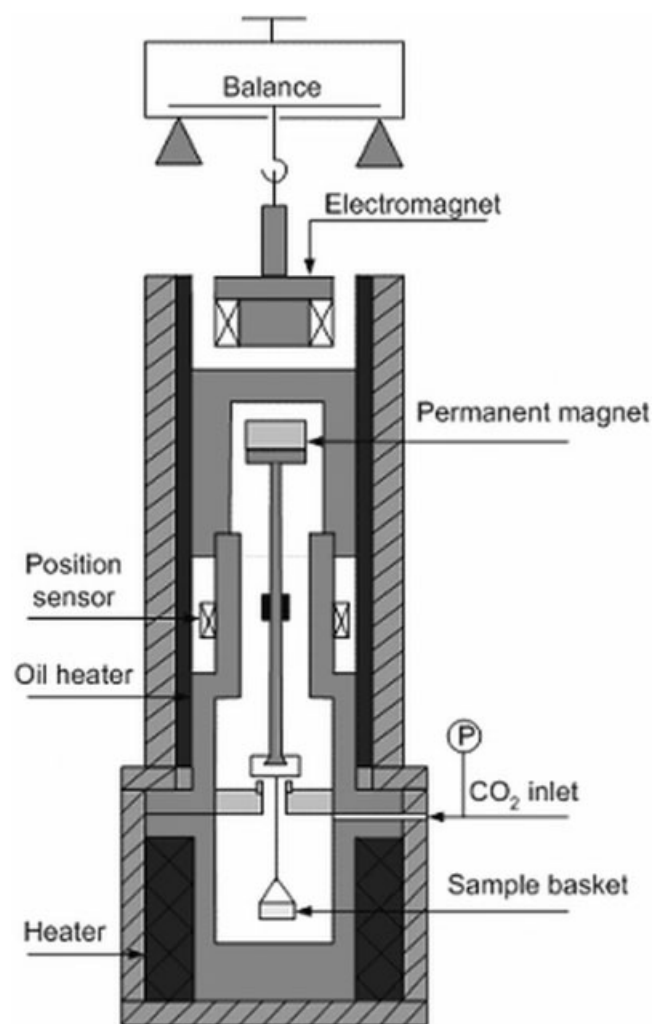


FIG. 1. The MSB apparatus used for the solubility measurements.

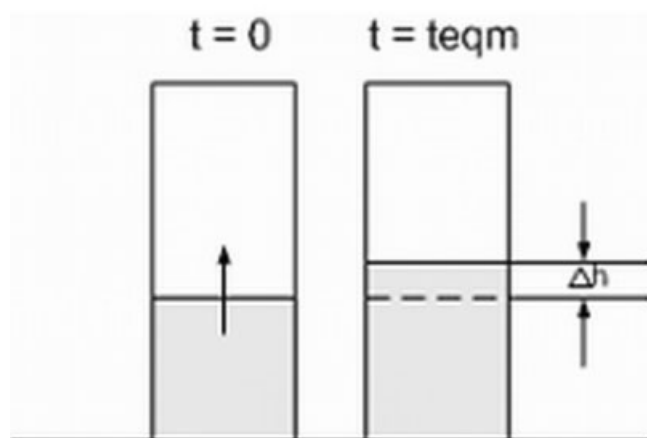
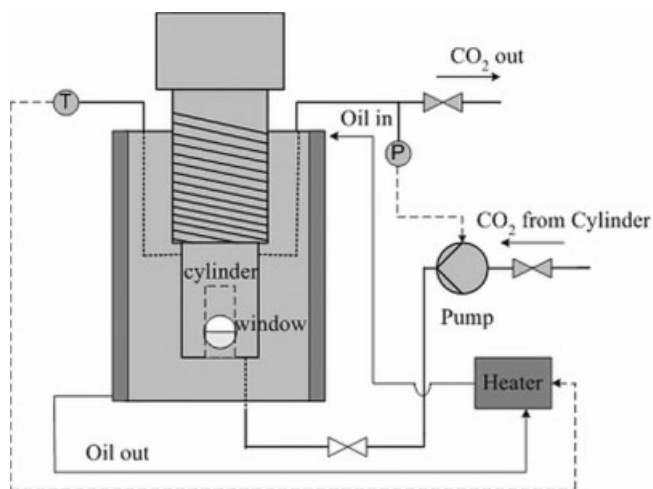


FIG. 2. (a) The optical cell used for measuring the swelling of a polymer. (b) The one-dimensional swelling of a polymer.

ence) before the final reading was recorded. Subsequently, more  $\text{CO}_2$  was introduced to attain a higher pressure and the new reading was recorded after equilibrium. Thus, solubility isotherms (without swelling correction) as a function of pressure were obtained.

**Optical Cell.** A high-pressure optical cell used for swelling measurements is shown in Fig. 2. The cell can be used at temperatures up to 473 K and pressures up to 35 MPa. The inner volume of the cell was 20 ml. The temperature of the cell was controlled within 0.1 K using an oil bath.  $\text{CO}_2$  was pumped to the cell at elevated pressures using an HPLC pump. A small glass cuvette having a square cross section was used for holding a polymer sample. In the cuvette, the swelling of the polymer occurred only in one direction as the other directions were confined by the walls of the cuvette as shown in Fig. 2. The swelling of the polymer was viewed through a quartz window of the optical cell. A cathetometer having a precision of 0.01 mm was used to measure the difference in the height of the sample from which a fractional change in the volume of the polymer was calculated.

Here, the change in the volume of the polymer sample is

termed as fractional swelling,  $\Delta V/V_0$ .  $\Delta V$  and  $V_0$  are the increment in the volume of the polymer sample due to swelling and the volume of the polymer sample in the absence of dissolved  $\text{CO}_2$ , respectively.

It can be seen from Eq. 1 that the data obtained using an MSB are not sufficient to calculate the solubility. Therefore, swelling measurements were carried out separately. For these measurements, a sample was prepared by pouring a molten polymer into a mould having a shape similar to the cuvette. After weighing the molded sample, it was fitted into the cuvette. The sample was again heated slightly above its  $T_g$  and pressed against the cuvette walls by a metal rod. The cylinder was then kept inside the cell and was heated to the desired temperature for about 3 h. Subsequently, the polymer surface was marked with a cathetometer followed by the addition of  $\text{CO}_2$  to the desired pressure. Due to a rapid initial swelling, it was difficult to mark the surface immediately after the addition of  $\text{CO}_2$  with the cathetometer. Pressure–volume–temperature (PVT) data of the polymer (i.e., specific volume of the polymer) were used to correct the initial cathetometer reading. The sample was then allowed to attain equilibrium. As the sorption equilibrium was reached, no further swelling of the polymer occurred. Then, the new surface was marked with the cathetometer. The difference in the sample volume was used to calculate the swelling of the polymer. For subsequent measurements at higher pressures, an additional amount of  $\text{CO}_2$  was introduced stepwise and a similar procedure was adopted.

The PVT data of the polymers were obtained using a high-pressure GNOMIX PVT apparatus (Datapoint Labs, USA) for a temperature range from 317 to 473 K and pressures up to 40 MPa. The PVT data of  $\text{CO}_2$  were obtained from the Span and Wagner EOS [11].

**Sanchez–Lacombe Equation of State.** To predict the solubility of  $\text{CO}_2$  at equilibrium conditions, the S-L EOS was used. Measured solubilities of sub- and supercritical  $\text{CO}_2$  in various polymers have successfully been correlated to the S-L EOS [6–8]. According to this theory, the polymer molecules are ordered according to a lattice structure. The theory accounts for the change in volume due to the presence of “holes” in the lattice, and hence, it does not require separate parameters to account for the flexibility of the molecule. The S-L EOS is given by:

$$\tilde{\rho}^2 + \tilde{P} + \tilde{T}[\ln(1 - \tilde{\rho}) + (1 - 1/r)\tilde{\rho}] = 0 \quad (2)$$

$$\tilde{v} = 1/\tilde{\rho} \quad (3)$$

where  $\tilde{\rho}$ ,  $\tilde{v}$ ,  $\tilde{P}$ ,  $\tilde{T}$  and  $r$  are the reduced density, specific volume, pressure, temperature, and the number of the lattice sites occupied by a molecule, respectively. An assumption used in the S-L EOS is that the polymer is monodisperse. The reduced parameters are defined as

$$\begin{aligned}
\tilde{\rho} &= \rho/\rho^* \\
\tilde{v} &= v/v^* \\
\tilde{P} &= P/P^* \\
\tilde{T} &= T/T^* \\
r &= MP^*/RT^*\rho^*
\end{aligned}
\quad (4)$$

where  $\rho^*$  (the corresponding mass density in the close-packed state at 0 K),  $v^*$  (the corresponding specific volume in the close-packed state),  $P^*$  (the hypothetical cohesive energy density in the close-packed state), and  $T^*$  (related to the depth of the potential energy well) are the characteristic parameters of components. These parameters are obtained by fitting PVT data of pure components using Eqs. 2–4 [12].

The EOS used for a mixture is similar to Eq. 2. The characteristic parameters used in the EOS for a mixture are obtained using the following mixing rules.

$$P^* = \sum_i \sum_j \phi_i \phi_j P_{ij}^* \quad (5)$$

$$P_{ij}^* = (1 - k_{ij})(P_i^* P_j^*)^{0.5} \quad (6)$$

$$T^* = P^* \sum_i (\phi_i^0 T_i^*) / P_i^* \quad (7)$$

$$r_i^0 v_i^* = r_i v_i^* \quad (8)$$

$$v^* = \sum_i \phi_i^0 v_i^* \quad (9)$$

$$1/r = \sum_i \phi_i / r_i \quad (10)$$

$$\phi_i^0 = (\phi_i P_i^* T_i^*) / \sum_j (\phi_j P_j^* T_j^*) \quad (11)$$

$$\phi_i = (w_i \rho_i^*) / \sum_j (w_j \rho_j^*) \quad (12)$$

where  $\phi$  and  $w$  represent the volume and weight fraction of components in two phases, respectively. Superscript “0” denotes the pure state of a component. Along with Eqs. 1–12, the chemical potential ( $\mu$ ) of a component in the available phases is used to predict the solubility of CO<sub>2</sub> in a polymer. At equilibrium,

$$\mu_i^{\text{gas}} = \mu_i^{\text{polymer}} \quad (13)$$

Here, CO<sub>2</sub> is termed as component “1” while a polymer as component “2.” The chemical potential of 1 in the polymer phase is given by

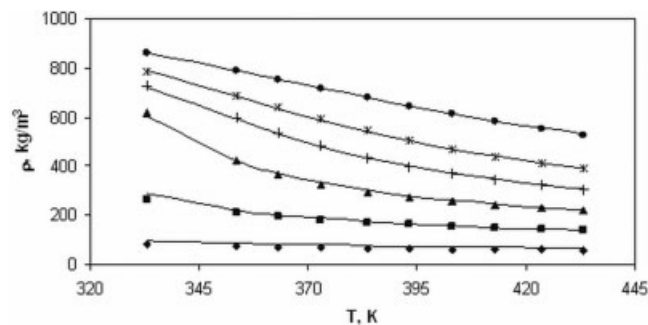


FIG. 3. Prediction of the densities of CO<sub>2</sub> using the S-L EOS: (◆) 4.5 MPa, (■) 10 MPa, (▲) 15 MPa, (+) 20 MPa, (\*) 30 MPa, and (●) 35 MPa. Solid symbols and solid lines denote the data obtained from Span and Wagner EOS and the data predicted using S-L EOS, respectively.

$$\begin{aligned}
\mu_1^{\text{polymer}} = RT[\ln \phi_1 + (1 - r_1/r_2)\phi_2 + r_1^0 \tilde{\rho} \phi_2^2 ((P_1^* + P_2^* \\
- 2P_{12}^*)/(P_1^* \tilde{T}_1))] + r_1^0 RT[-\tilde{\rho}/T_1 + \tilde{P}_1 \tilde{v}/\tilde{T}_1 \\
+ \tilde{v}((1 - \tilde{\rho})\ln(1 - \tilde{\rho}) + \tilde{\rho}/r_1^0 \ln \tilde{\rho})]. \quad (14)
\end{aligned}$$

Equation 14 is also used to calculate  $\mu_1^{\text{gas}}$  by considering only the gas phase. For polymers of high molecular weight, it is safe to assume that no polymer is present in the gas phase. Thus, the experimental solubility data are regressed with an adjustable interaction parameter,  $k_{ij}$ , which measures the deviation of  $P_{ij}$  from the geometric mean of  $P_i$  and  $P_j$  using Eqs. 2–14.

## RESULTS AND DISCUSSION

The PVT data of the polymers and CO<sub>2</sub> are essential for the interpretation of the swelling measurements and in the S-L EOS as discussed above. Therefore, the PVT and swelling studies are described before the solubility results. The PVT data have been successfully modelled using the S-L EOS for a wide range of temperatures, pressures, and densities. The results for CO<sub>2</sub>, PPB and PEB are shown in Figs.

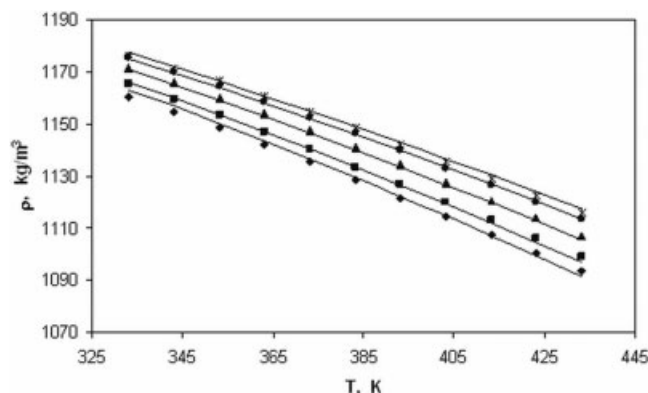


FIG. 4. Prediction of the densities of PPB using the S-L EOS: (◆) 4.5 MPa, (■) 10 MPa, (▲) 20 MPa, (●) 30 MPa, and (\*) 35 MPa. Solid symbols and solid lines denote the experimental data and the data predicted using S-L EOS, respectively.



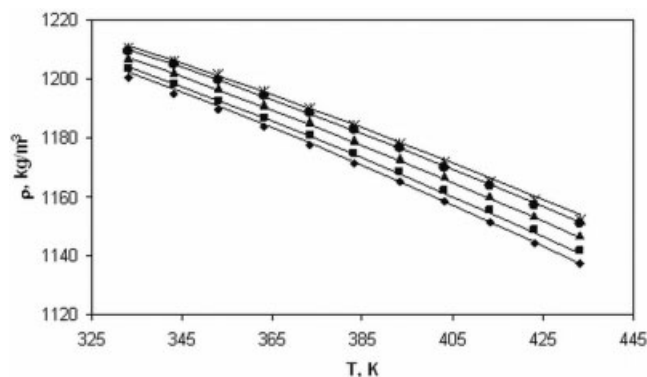


FIG. 5. Prediction of the densities of PEB using the S-L EOS. (◆) 4.5 MPa, (■) 10 MPa, (▲) 20 MPa, (●) 30 MPa, and (\*) 35 MPa. Solid symbols and solid lines denote the experimental data and the data predicted using S-L EOS, respectively.

3, 4, and 5, respectively. The characteristic parameters of the pure components, obtained using the S-L EOS are given in Table 2. These parameters have been used to calculate the solubility.

When CO<sub>2</sub> is dissolved into a polymer, the mobility of the polymer chains is increased due to disentanglement of the polymeric chains. As a result, the free volume inside the polymer is increased and swelling of the polymer takes place. Experimentally obtained swelling isotherms of PPB and PEB in the presence of CO<sub>2</sub> using the optical cell apparatus are shown in Figs. 6 and 7, respectively. It can be seen from these figures that the fractional swelling is increased with increasing pressure for both PPB and PEB. In general, the higher the dissolved amount of CO<sub>2</sub> in a polymer the larger is the swelling of the polymer. This effect is the result of increasing CO<sub>2</sub> density upon an increase in pressure. Since the CO<sub>2</sub> density decreases with temperature, a reduction in the swelling is expected at higher temperatures in both polymers. However, this is observed only for PPB. The swelling of PEB increases with increasing temperature. This inverse swelling behavior has also been reported for poly (dimethyl siloxane) (PDMS), poly (ethylene-terephthalate) (PET), and bisphenol-A polycarbonate (PC) [13, 14]. It has been suggested that the CO<sub>2</sub> density is not the only parameter, which affects the swelling of the polymer. A positive temperature influence on chain mobility is pronounced compared to the influence of CO<sub>2</sub> density for an inverse swelling behavior [14]. This effect is not present in PPB, which is most probably caused by an easily accessible free volume due to its low molecular weight.

TABLE 2. Characteristic parameters of the polymers and CO<sub>2</sub> obtained using the S-L EOS.

Component	$P^*$ (MPa)	$T^*$ (K)	$\rho^*$ (kg/m <sup>3</sup> )
CO <sub>2</sub>	427.7	338.7	1405.5
PPB	439.7	683.2	1242.7
PEB	640.2	728.6	1271.0

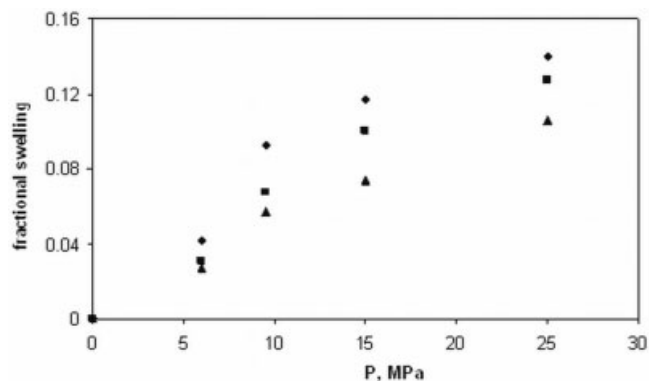


FIG. 6. Fractional swelling isotherms of PPB in the presence of CO<sub>2</sub>. (◆) 333 K, (■) 368 K, and (▲) 420 K.

CO<sub>2</sub> solubilities in both polymers have been measured and have correlated with the S-L EOS. The results are shown in Figs. 8 and 9. The experimental data from the MSB are corrected for buoyancy effects using the results of the swelling measurements. The CO<sub>2</sub> solubility is represented in terms of the weight fraction of CO<sub>2</sub> dissolved in the polymer. The solubilities of CO<sub>2</sub> have been corrected with the experimental swelling data. For both polymers, it is found that the solubility increases with increasing pressure, whereas it decreases with increasing temperature. This relates to high CO<sub>2</sub> densities at high pressures and low temperatures, and vice versa. At a low temperature, around 333 K, the solubility behavior is not linear above 15 MPa for both polymers. Probably at elevated pressures, the free volume available in the polymer is reduced due to compression of the polymer. Such effects are more pronounced at the low temperature due to relatively small free volume. Moreover, Figs. 8 and 9 also show that this nonlinear behavior is absent at high temperatures.

The CO<sub>2</sub> solubilities in PPB are higher than that in PEB. The importance of the free volume available in the polymer [15] and minor changes in the groups present in a polymer [16, 17] for the CO<sub>2</sub> solubility has already been discussed in the literature. As the structure is nearly similar for both polyesters, the accessible free volume in PEB that is smaller

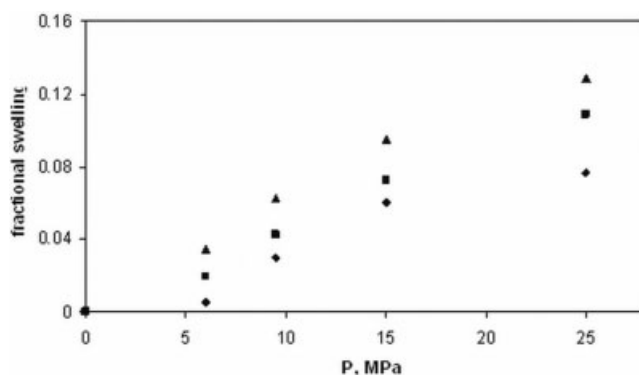


FIG. 7. Fractional swelling isotherms of PEB in the presence of CO<sub>2</sub>. (◆) 334 K, (■) 373 K, and (▲) 418 K.

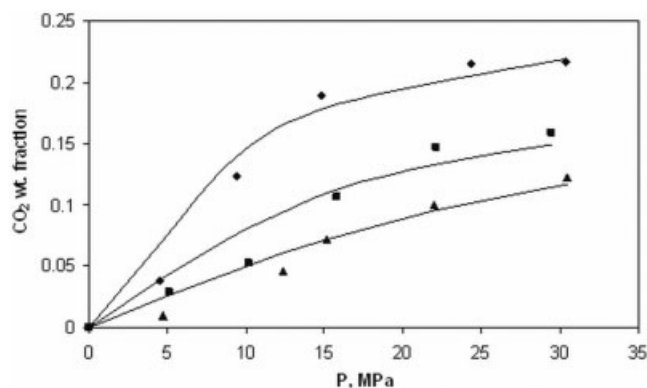


FIG. 8. The  $\text{CO}_2$  solubility isotherms of PPB.  $k_{12}$  (( $\blacklozenge$ ) 333 K) = 0.065,  $k_{12}$  (( $\blacksquare$ ) 368 K) = 0.09, and  $k_{12}$  (( $\blacktriangle$ ) 420 K) = 0.108. Solid symbols and solid lines denote the experimental data and the data predicted using S-L EOS, respectively.

due to higher chain entanglements (high molecular weight) is responsible for different solubility. The higher chain entanglements compared to PPB make  $\text{CO}_2$  more difficult to access the carboxyl groups in PEB than in PPB. Albeit the swelling increases with an increase in temperature in PEB, the low  $\text{CO}_2$  densities at high temperatures reduce the solubility.

The solubility results have been correlated with the S-L EOS for both PPB and PEB (see also Figs. 8 and 9) respectively. To fit the S-L EOS to the experimental solubility data, Eqs. 2–14 have been solved using the characteristic parameters determined from the PVT data (Table 2). A nonlinear regression optimization procedure (Levenberg-Marquardt, MATLAB 7) has been used for minimizing the difference between the chemical potential of  $\text{CO}_2$  in the gas phase and the polymer phase, and also between the experimental and predicted solubilities using the interaction parameter,  $k_{12}$ . It can be seen from Figs. 8 and 9 that the S-L EOS is a good tool for predicting the  $\text{CO}_2$  solubility in PPB and PEB. Though the S-L EOS has already been reported for several polymers to predict the swelling due to dissolved

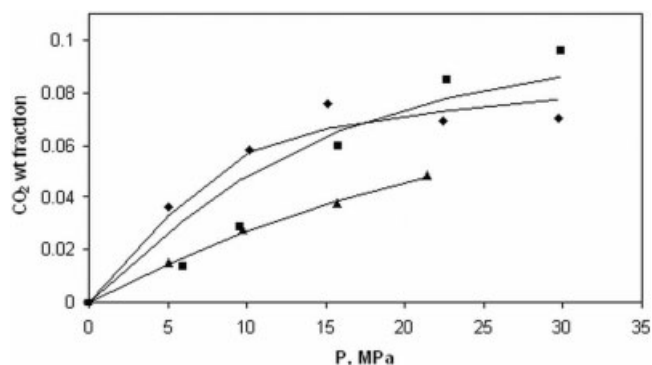


FIG. 9. The  $\text{CO}_2$  solubility isotherms of PEB.  $k_{12}$  (( $\blacklozenge$ ) 334 K) = 0.091,  $k_{12}$  (( $\blacksquare$ ) 373 K) = 0.083, and  $k_{12}$  (( $\blacktriangle$ ) 418 K) = 0.119. Solid symbols and solid lines denote the experimental data and the data predicted using S-L EOS, respectively.

$\text{CO}_2$ , it has not been tested together with the experimental swelling and solubility data for molten polymers. The density of a mixture can be determined using the S-L EOS, which has been used to predict the swelling of both polymers. The swelling has been poorly predicted by this EOS for PPB and PEB. The linear mixing rule for the volume of the mixture in the S-L EOS may be responsible for this poor predictability. Royer et al. [13] have introduced a correction parameter in the mixing rule used for the volume in the S-L EOS to predict the swelling of and the solubility of  $\text{CO}_2$  in PDMS. Recently, over prediction of swelling using the S-L EOS has been reported for EVA polymers by Jacobs et al. [18].

## CONCLUSIONS

The solubilities of  $\text{CO}_2$  in PPB and PEB in the molten state have been measured using the MSB. It appeared to be necessary to correct the data obtained from the MSB with independent swelling data. The polymers swell considerably in the presence of  $\text{CO}_2$  when they are exposed to elevated pressures. The  $\text{CO}_2$  solubility in the polymers increases with an increase in pressure and decreases with an increase in temperature. The  $\text{CO}_2$  solubility in PEB is lower than that in PPB, which is probably due to its smaller accessible free volume as a result of the higher molecular weight. Around 333 K, a nonlinear trend for solubility–pressure has been observed at elevated pressures for both polymers due to compression effect. The experimental solubility data have been correlated with the S-L EOS using the pure component parameters and an adjustable interaction parameter. Although the S-L EOS has often been used to predict the swelling of a polymer in the presence of  $\text{CO}_2$ , it is not valid for the polymers investigated here.

## ACKNOWLEDGMENTS

This research was supported by the Technology Foundation STW, applied science division of NWO and the technology programme of the Ministry of Economic Affairs.

## REFERENCES

1. M. Perrut and J. Jung, *J. Sup. Fluids*, **20**, 179 (2001).
2. V. Wiesmet, E. Weidner, S. Behme, G. Sadowski, and W.J. Arlt, *J. Sup. Fluids*, **17**, 1 (2000).
3. Y. Sato, M. Yurugi, K. Fujiwara, S. Takishima, and H. Masuoka, *Fluid Phase Equil.*, **125**, 129 (1996).
4. Y. Kamiya, K. Mizoguchi, K. Terada, Y. Fujiwara, and J.-S. Wang, *Macromolecules*, **31**, 472 (1998).
5. R. Kleinrahm and W. Wagner, *J. Chem. Therm.*, **18**, 739 (1986).
6. Y. Sato, T. Takikawa, A. Sorakubo, S. Takishima, H. Masuoka, and M. Imaizumi, *Ind. Eng. Chem. Res.*, **39**, 4813 (2000).

7. Y. Sato, T. Takikawa, S. Takishima, and H. Masuoka, *J. Sup. Fluids*, **19**, 187 (2001).
8. Y. Sato, T. Takikawa, M. Yamane, S. Takishima, and H. Masuoka, *J. Sup. Fluids*, **194**, 847 (2002).
9. I.C. Sanchez and R.H. Lacombe, *J. Phys. Chem.*, **80**, 2352 (1976).
10. I.C. Sanchez and R.H. Lacombe, *Macromolecules*, **11**, 1145 (1978).
11. R. Span and W. Wagner, *J. Phys. Chem. Ref. Data*, **25**, 1509 (1996).
12. A. Garg, E. Gulari, and C.W. Manke, *Macromolecules*, **27**, 5643 (1998).
13. J.R. Royer, J.M. DeSimone, and S.A. Khan, *Macromolecules*, **32**, 8965 (1999).
14. J.V. Schnitzler and R. Eggers, *J. Sup. Fluids*, **16**, 81 (1999).
15. V.M. Shah, B.J. Hardy, and S.A. Stern, *J. Polym. Sci.: Polym. Phys.*, **31**, 313 (1993).
16. S.G. Kazarian, M.F. Vincent, and C.A. Eckert, *Rev. Sci. Instrum.*, **67**, 1586 (1996).
17. S.G. Kazarian, M.F. Vincent, F.V. Bright, C.L. Liotta, and C.A. Eckert, *J. Am. Chem. Soc.*, **118**, 1729 (1996).
18. M.A. Jacobs, M.F. Kemmere, and J.T.F. Keurentjes, *Polymer*, **45**, 7539 (2004).